Nanoscale Res Lett (2009) 4:1463–1468
DOI 10.1007/s11671-009-9421-8

NANO EXPRESS

Rolled-Up Nanotech: Illumination-Controlled Hydrofluoric Acid Etching of AlAs Sacrificial Layers

Ruxandra M. Costescu · Christoph Deneke · Dominic J. Thurmer · Oliver G. Schmidt

Received: 2 June 2009 / Accepted: 14 August 2009 / Published online: 3 September 2009

Abstract The effect of illumination on the hydrofluoric acid etching of AlAs sacrificial layers with systematically varied thicknesses in order to release and roll up InGaAs/GaAs bilayers was studied. For thicknesses of AlAs below 10 nm, there were two etching regimes for the area under illumination: one at low illumination intensities, in which the etching and releasing proceeds as expected and one at higher intensities in which the etching and any releasing are completely suppressed. The "etch suppression" area is well defined by the illumination spot, a feature that can be used to create heterogeneously etched regions with a high degree of control, shown here on patterned samples. Together with the studied self-limitation effect, the technique offers a way to determine the position of rolled-up micro- and nanotubes independently from the predefined lithographic pattern.

Keywords Rolled-up · Nanotubes · Nanotech · Nanostructures · Etching · Hydrofluoric acid · III–V layers · Illumination-controlled

Introduction and Background

Rolled-up nanotech [1, 2] has become a powerful technology with applications in a broad range of research fields, including optofluidics [3], micromachinery [4–6], magnetofluidics [4, 7], biophysics [4, 8], nanomechanics [9], and waveguiding for different spectral ranges and applications [10–12]. Large arrays of periodically ordered microtubes can be fabricated by a combination of lithography and deliberate self-rolling of strained layers upon selective underetching [1, 13–15]. However, in some cases, it might be important to stimulate tube formation in certain areas and suppress tube formation outside those areas. Precise control over the lateral positioning and the number of windings is fundamental for the use of the tubes in optical resonators for sensors [16–20], hyperlenses [4, 21, 22], or electrical transport (curved electron gases) [23–27]. Numerous existing studies offer highly sophisticated methods for precise lateral positioning of rolled-up semiconductor nanostructures by controlling the starting edges [13–15, 28, 29], but difficulties arise for thin layers due to the extensive, successive lithography steps involved, and ways to control the stopping point of rolling remain largely lacking without modifying the structure.

Here, we demonstrate illumination-controlled hydrofluoric acid (HF) etching of a buried thin AlAs sacrificial layer. Sufficiently intense light exposure of a certain substrate area leads to a complete suppression of the underetching effect, and as a result, the formation of rolled-up InGaAs/GaAs tubes can be easily controlled spatially. This method allows for control over the roll-up stopping point and is suitable for very thin sacrificial layers.

The aim of this study was to quantify the observed "etch-suppression effect" (ESE) and precisely control the release of InGaAs/GaAs bilayers with an illumination technique.

Experimental Details

Figure 1a shows schematically the formation process of a III–V rolled-up nanotube (RUNT): when immersed in HF

R. M. Costescu (✉) · C. Deneke · D. J. Thurmer · O. G. Schmidt
Institute for Integrative Nanosciences, IFW Dresden, Helmholtzstr. 20, 01069 Dresden, Germany
e-mail: r.costescu@ifw-dresden.de

solution, the compressively strained double layer (a GaAs layer on top of a larger-lattice constant In_xGa_{1-x} As layer deposited pseudomorphically on a GaAs substrate with an AlAs sacrificial layer) releases from the substrate as the sacrificial layer is preferentially removed by the HF at a previously defined starting edge and begins to roll up in order to relax the built-in strain gradient. Finally, the bent bilayer forms a tube or scroll after performing a full rotation. The starting edge, which for InGaAs/GaAs layers should be oriented in the [100] direction for optimal structural integrity of the resulting RUNTs [29, 30], can be defined either by scratching the surface, thereby laterally exposing the sacrificial layer, or by opening a window through the entire layer structure by photolithography and subsequent wet chemical etching. The tube diameter, i.e., the size of the cross section of the structure obtained after the etching step has been completed, depends on the thickness and inherent strain of the layers, and can be accurately varied in the nano- to micrometer range [1, 30, 31, 32]. For precise positioning of RUNTs on the surface, the important parameters in the roll-up process are the sacrificial layer thickness, etching time, and tube diameter [30]. The ratio of inner-to-outer diameter can also be controlled over a wide range, based on the number of rotations performed by the tubes on the surface (or rolling distance, measured from the initial starting edge—see schematic in Fig. 1a, step 3 and Fig. 3, inset) [30].

Here, the experiments were performed using 20 nm $In_{0.33}Ga_{0.66}As$/20 nm GaAs structures on AlAs grown on (001) GaAs substrates by molecular beam epitaxy, where the thickness of the AlAs was varied from 4 to 20 nm. For experiments pertaining to the measurement of the onset of the etch suppression and rolling distance, the starting edges were defined by mechanical scratching, whereas photolithography and wet chemical etching (by H_3PO_4:H_2O_2:H_2O solution) were used for controlling the etch suppression. Our specially designed setup involved an HF-resistant trough for etching with HF under light focused by a Zeiss optical microscope using different objective lenses of 5 × through 50 × magnification (for sample evolution during this process, see Fig. 1a and b). Other measurements were performed using illumination from a HeNe laser with maximum output power of 2 mW, as well as a laser with adjustable power (up to 20 mW) and wavelength (535–825 nm) with focusing optics or an optical fiber to illuminate the surface of the sample. For all measurements, the intensity of illumination was measured beforehand using a calibrated power meter. For samples that were etched, illuminated, and observed under the microscope, the settings on the illumination dial were used and the focused spot sizes for each magnification were assumed to be the same. For the quantitative measurements of tube rolling distance, optical images of the sample outside of solution once the etching was terminated were taken. From these

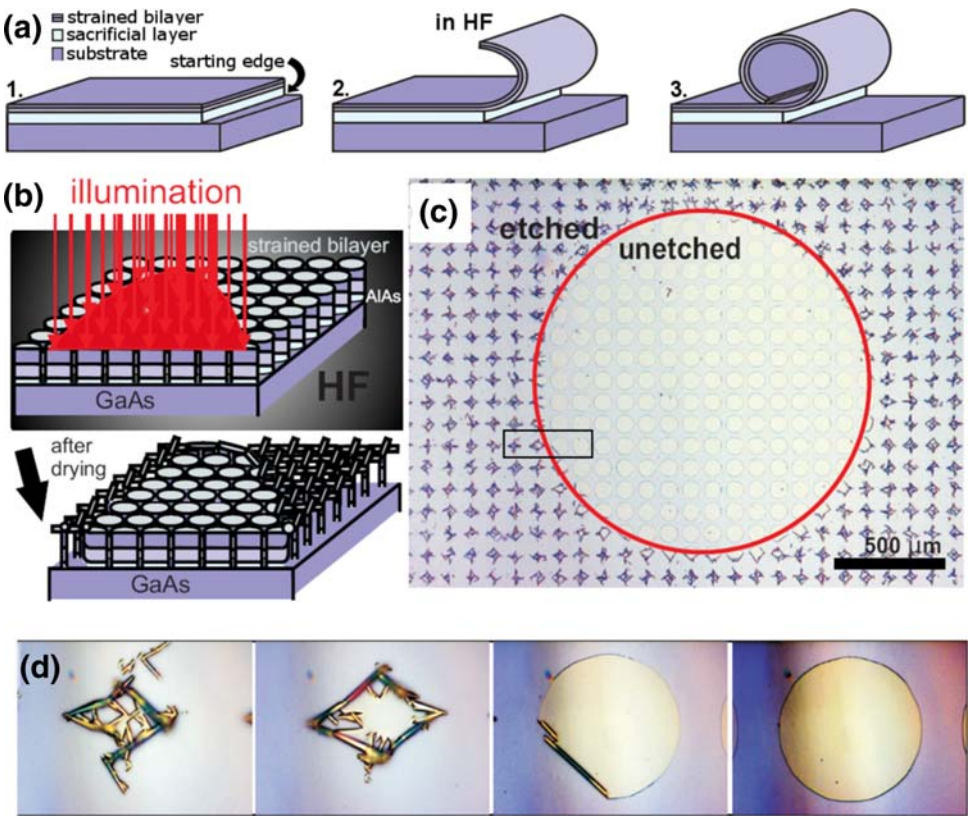

Fig. 1 **a** Steps of strained bilayer roll-up process (*1*. initial strained bilayer/sacrificial layer/substrate structure with defined starting edge, *2*. bilayer rolling due to sacrificial layer removal in HF, *3*. rolled-up structure after one full rotation). **b** Schematic of the etching experiment during in situ observation by optical microscopy and result for strained bilayers (relative ratio of mesa diameter to layer thickness not to size). **c** Optical image of an AlAs/InGaAs/GaAs mesa structure etched in a 2.5% HF solution, with 20 × microscope objective, for 6 min; the etch-suppression spot radius is ∼700 µm. **d** Optical images of adjacent mesas from (**b**) (*black box*), showing an increasing degree of etch suppression toward the center of the illumination

images, the rolling distance could then be measured, which we define as distance from the starting edge to the center of the tube width, assumed to correspond to the stopping point of the underetching.

The resolution of the ES method was studied by precisely positioning the illumination spot on wet-chemically etched mesa structures of different shapes and sizes (on the order of 10–100 μm) during HF etching. The degree of etching suppression (given by the coverage area of unetched structures remaining on the sample) was measured versus distance from the center of illumination.

Results

Characteristics of Etching Suppression Effect

Figure 1b shows an optical microscopy image of a structure composed of a 4 nm AlAs layer and a 40 nm symmetrical strained $In_{0.33}Ga_{0.66}As$/GaAs bilayer. The larger circular shape observed on the sample at the end of the HF experiment is formed by original mesa structures that were left unetched, while on the rest of the sample the bilayer mesas are underetched, leading to rolling up as expected.

Figure 2, which plots the average rolling distance as a function of intensity for structures with varying AlAs thickness, illustrates the sudden onset of the ESE. The error due to variations in experimental parameters such as quantity of HF solution, scattering of light and effective illumination intensity at the sample, as well as the method for evaluating rolling distances, is estimated to be within 15%. It can be seen that the maximum rolling distance increases as the AlAs thickness increases, while the ESE is only present for sacrificial layers below 10 nm. Moreover, the onset of the ESE, or the intensity of illumination necessary to suppress the AlAs etching, is higher for larger thicknesses.

Figure 3 shows the maximum rolling distance as a function of the sacrificial layer thickness. In a regime from 5 nm up to a thickness of 15 nm of AlAs the relationship between the maximum rolling distance and the sacrificial layer thickness is approximately linear, and then saturates for thicker AlAs layers. Although in previous studies [14, 30] InGaAs-GaAs RUNTs (rolled-up nanotubes) have been noticed to exhibit a self-limiting rolling behavior for longer etching times, this limiting was not investigated as function of the sacrificial layer thickness. The fit through the data in the linear increase regime ($R^2 = 0.936$) yields a unitless slope of $14.2e^3$ for the scaling of maximum rolling distance with t_{AlAs}. This indicates that in this first regime the maximum rolling distance is not dominated by intrinsic effects of the rolled-up layer and does not occur due to a fundamental limiting process (as, e.g., described by Cendula et. al. [33]). Therefore, we ascribe the saturation in this regime to dynamic effects either between the rolled-up layer and the substrate or inside the etching solution caused by the process in the gap between the substrate and the rolled-up film. The second regime shows a clear saturation behavior for AlAs thickness larger than 15 nm. In this

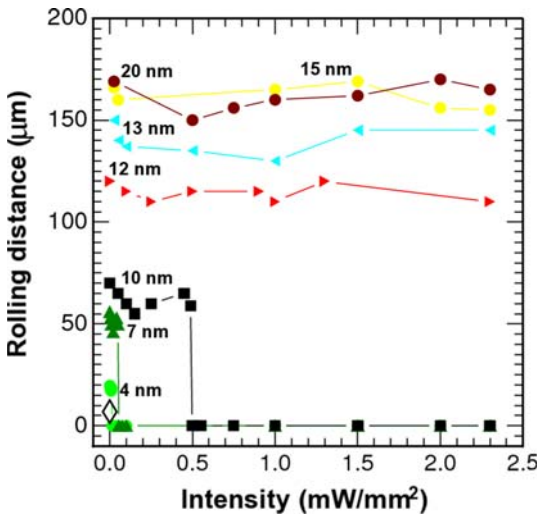

Fig. 2 Onset of illumination effect for 20 nm InGaAs/20 nm GaAs samples with 4, 7, 10, 12, 13, 15, and 20 nm AlAs sacrificial layers, etched with 2.5% HF solution using 20 × microscope objective, for 8 min; the starting edges were produced by mechanical scratching. The diamond data point shows a maximum rolling distance previously reported [14]

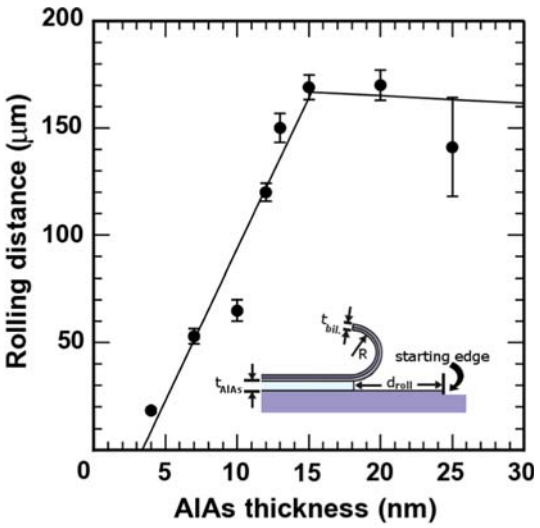

Fig. 3 Maximum rolling distance versus various AlAs thicknesses (same parameters as in Fig. 2); the starting edges were produced by mechanical scratching. The *line* through the data in the linear increase regime is a best fit. The inset shows a cross section of step 2 in Fig. 1a, indicating rolling distance d_{roll} measured from the starting edge, AlAs thickness t_{AlAs}, InGaAs/GaAs bilayer thickness $t_{bil.}$, and radius of curvature R of the rolled-up bilayer

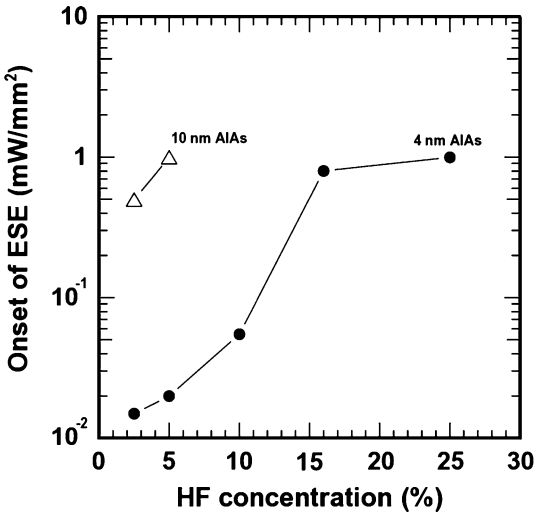

Fig. 4 The onset of the etch-suppression effect (ESE) versus HF concentration for 20 nm InGaAs/20 nm GaAs structures with 4 nm and 10 nm AlAs sacrificial layers, with 20 × microscope objective, for 8 min; the starting edges were produced by mechanical scratching. The *lines* through the data are guides for the eye

regime, the saturation should be dominated by intrinsic effects either from the layer system itself or possibly by some kind of fundamental process yet to be found. The linear scaling of the maximum rolling distance offers the possibility for lateral positioning of the rolled-up tube relative to a defined starting edge [14].

Furthermore, as shown in Fig. 4, the onset of ESE changes for different etching speeds: the higher the HF concentration, the higher the intensity needed for suppression, while the thicker the AlAs layer, the more abrupt the etching behavior transition from the "suppression regime" to the "illumination independent regime." For each t_{AlAs}, up to roughly 15 nm the onset of the ESE increases approximately linearly with concentration, and scaling slopes are comparable for different thicknesses (≈ 12 mW/mm^2). From this, as well as Fig. 2, it can be concluded that the onset of ESE occurs in a different regime from that of intrinsic saturation of maximum rolling distance.

We also found that the ESE is time dependent, i.e., the etching time under illumination determines whether further etching will continue once the illumination is removed. In our experiments, we found that for samples where the high intensity light exposure was kept short, the layers were able to start rolling after being removed from the light source. This effect was found to not only depend on the light intensity but also on the thickness of the AlAs layer, which suggests that the etch suppression is a dynamic process that depends on the access of HF to the AlAs layer and the exchange of products and reactants in this region. This conclusion is further corroborated by the fact that with increasing AlAs thickness the rolling distance of the strained bilayer becomes independent of the AlAs gap size (Fig. 3).

Using Etch Suppression for Nanotube Positioning

The ESE was used to position and control the roll up of tubes from strained InGaAs/GaAs bilayers. The patterning allowed us to create well-defined starting edges suitable for the illumination experiment (as in Fig. 1). By cleverly integrating this process, one can obtain both etched regions with rolled-up layers and unetched regions within a small area on the sample. Furthermore, this technique is useful for applications since, during the ES, the structures remain unchanged other than the "blocking" at the starting edge.

The resolution of this method is indicated by Fig. 5, which is a plot of the degree of etching/suppression versus the distance from the center of the illumination for the 80-μm diameter pattern shown in Fig. 1. The "degree of etch suppression" is the percentage of the circular mesa surface, which appears intact in optical images of the etched structures (see Fig. 1d). As can be seen from this plot, the length scale on which the ESE transitions from "no significant suppression" to "full suppression" is ~100 μm. Further refinement is possible either using smaller illumination areas, restricting light access close to the surface of the samples (for instance, by a shadow mask placed directly above the sample in the solution) or developing

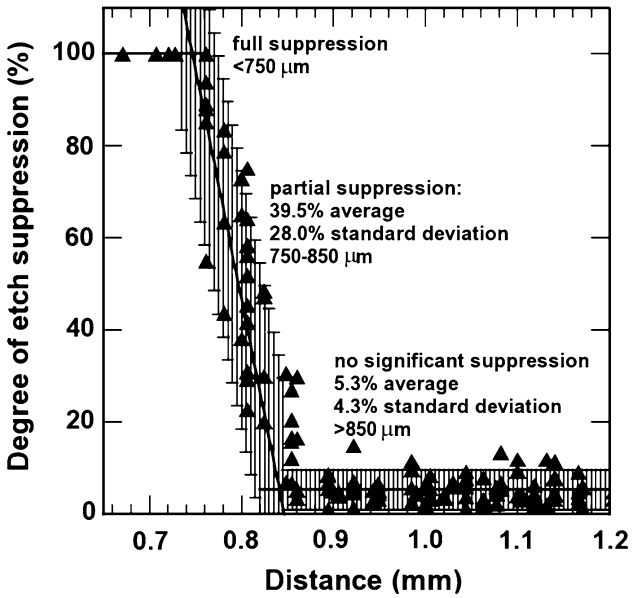

Fig. 5 "Degree of suppression" (% of area) versus distance from the center of the illumination for the sample in Fig. 1. The *grey* areas indicate a fit based on the average degree of suppression and standard deviation values, for all points below and above a distance of 850 μm, differentiating the regimes with ESE and no significant ESE, respectively

methods to reduce stray light and diffraction in the solution.

Discussion, Uncertainties, and Limitations

We investigated the rolling distance as a function of illumination intensity used during the HF etching of AlAs/InGaAs/GaAs structures on GaAs for different sacrificial layer thicknesses. For AlAs layers thinner than 10 nm, total suppression of the etching process occurs beyond a threshold intensity that increases with increasing AlAs thickness.

The ESE is clearly influenced by the AlAs-HF reaction rate as well as the physical characteristics of the structure: the larger the sacrificial layer gap and faster the reaction rate, the higher the intensity of illumination needed to suppress the etching. This trend continues up to a point where the reaction is no longer illumination dependent and suppression is no longer possible. A further series of experiments involving etching with filtered light and a focused laser beam of varying wavelengths (not presented here) suggests that the ESE is preserved for lower energies than the AlAs band gap and therefore any photochemical effect in HF cannot depend on light excitation of the AlAs material. We have also eliminated the possibility that heating plays a significant role in the ESE, since experiments that involve heating samples in HF solution past the boiling point show an enhancement rather than suppression of the etching and hence would counteract this effect.

We believe that for the ESE found in samples etched with HF for shorter times under illumination levels close to the threshold value from Fig. 2, the strained bilayer remains intact because the sacrificial layer was not underetched at the starting edge, which may happen through the accumulation of solid As and As oxide following from a photochemical interaction at the GaAs surface in the presence of HF.

The process through which AlAs sacrificial layers are wet-etched with hydrofluoric acid (HF) [34–43] as well as the laser-induced etching of semiconductors by a dilute acid solution [44–46] have been investigated previously in some depth. In HF-AlAs reactions, any passivating As formed at the surface is usually oxidized and then dissolved, thus allowing new access to the etch front and sustaining etching [34]. But if the rate of As production exceeds that of oxide formation, or if the type of oxide is stable in the HF, then the etching will be inhibited. From laser-induced etching studies, it is clear that porous stable oxide films formed at the semiconductor surface give a time dependence for the process [46]. During the redox reaction, As(III) must be complexed by water and dissolved as $HAsO_2$ and As_2O_3, but when the concentration of As(III) surpasses the solubility limit, there is precipitation of As at the surface, slowing down the reaction. Our results match well with this type of process, and we propose that the ESE occurs in a similar fashion: the formation of very small amounts of As or As_2O_3 at the AlAs gap, which would nonetheless be enough to block access of HF to films under 10 nm, can effectively suppress the underetching of the AlAs layer. In accordance with our findings, the thicker the sacrificial layer gap and the faster the HF etching rate, the less likely the ESE takes place. In the suppression regime for thinner AlAs layers, for higher intensities of illumination the photogeneration of holes is more pronounced leading to a faster subsequent passivation (and reaching of the ESE limit with time). For thicker AlAs layers, higher illumination can still lead to changes at the GaAs substrate interface [46] but does not hinder the etching of the AlAs.

Conclusion

While the self-limitation of the maximum rolling distance of RUNTs allows for the precise tuning of the number of rotations as a function of the sacrificial layer, the illumination permits the exact positioning of the tube in combination with common lithographic technology. Fine-tuning the etch suppression with patterned samples can yield a useful way of precisely controlling the roll up of strained InGaAs/GaAs bilayers and the entire tube fabrication process, as well as other more general laser-assisted microfabrication applications, with a convenient, customizable method. In this way, it is complementary to prepattering of the sample by lithographic means and allows for a full control over the position of the produced RUNTs.

Acknowledgments The authors would like to thank Emica Coric, Dr. Stefan Baunack, Dr. Jurgen Thomas, and Dr. Ingolf Monch for processing and characterization help, and Dr. Armando Rastelli and Dr. Francesca Cavallo for fruitful discussions.

References

1. V.Ya. Prinz, V.A. Seleznev, A.K. Gutakovsky, A.V. Chehovskiy, V.V. Preobrazhenskii, M.A. Putyato, T.A. Gavrilova, Physica E **6**(1–4), 828–831 (2000)
2. O.G. Schmidt, K. Eberl, Nature **410**(6825), 168 (2001)
3. A. Bernardi, S. Kiravittaya, A. Rastelli, R. Songmuang, D.J. Thurmer, M. Benyoucef, O.G. Schmidt, Appl. Phys. Lett. **93** 094106 (2008)
4. Y. Mei, G. Huang, A.A. Solovev, E. B. Urena, I. Mönch, F. Ding, T. Reindl, R.K.Y. Fu, P.K. Chu, O.G. Schmidt, Adv. Mat. **20**(21), 4085–4090 (2008)
5. L. Zhang, J.A. Abbott, L. Dong, B.E. Kratochvil, D. Bell, B.J. Nelson, Appl. Phys. Lett. **94**, 064107 (2009)
6. A.A. Solovev, Y. Mei, E. Bermudez Urena, G. Huang, O.G. Schmidt, Small, **5**, 1688 (2009)

7. E. Bermudez, Y. Mei, E. Coric, D. Makarov, M. Albrecht, O.G. Schmidt, J. Phys. D: Appl. Phys. **42**(5), 4085–4090 (2009)
8. G. Huang, Y. Mei, D.J. Thurmer, E. Coric, O.G. Schmidt, Lab Chip **9**, 263–268 (2009)
9. L. Zhang, L. Dong, B.J. Nelson, Appl. Phys. Lett. **92**, 243102 (2008)
10. S. Mendach, R. Songmuang, S. Kiravittaya, A. Rastelli, M. Benyoucef, O.G. Schmidt, Appl. Phys. Lett. **88**, 111120 (2006)
11. Ch. Deneke, O.G. Schmidt, Appl. Phys. Lett. **89**, 123121 (2006)
12. E.J. Smith, Z. Liu, Y. Mei, O.G. Schmidt, Nano Lett. (2009) doi:10.1021/nl900550j
13. A.B. Vorob'ev, V.Ya. Prinz, Semicond. Sci. Technol. **17**, 614–616 (2002)
14. C. Deneke, O.G. Schmidt, Appl. Phys. Lett. **85**, 2914 (2004)
15. X. Li, J. Phys. D: Appl. Phys. **41**, 193001 (2008)
16. T. Kipp, H. Welsch, Ch. Strelow, Ch. Heyn, D. Heitmann, Phys. Rev. Lett. **96**, 077403 (2006)
17. S. Mendach, S. Kiravittaya, A. Rastelli, M. Benyoucef, R. Songmuang, O.G. Schmidt, Phys. Rev. B **78**, 035317 (2008)
18. Ch. Strelow, H. Rehberg, C.M. Schultz, H. Welsch, Ch. Heyn, D. Heitmann, T. Kipp, Phys. Rev. Lett. **101**, 127403 (2008)
19. R. Songmuang, A. Rastelli, S. Mendach, T. Shigaki, Appl. Phys. Lett. **90**, 091905 (2007)
20. M. Hosoda, T. Shigaki, Appl. Phys. Lett. **90**, 181107 (2007)
21. S. Schwaiger, M. Broll, A. Krohn, A. Stemmann, C. Heyn, Y. Stark, D. Stickler, D. Heitmann, S. Mendach, Phys. Rev. Lett., **102**, 163903 (2009)
22. E.J. Smith, Z. Liu, Y.F. Mei, O.G. Schmidt, Appl. Phys. Lett., (2009, in press)
23. K.J. Friedland, R. Hey, H. Kostial, A. Riedel, K.H. Ploog, Phys. Rev. B **75**, 045426 (2007)
24. A.B. Vorob'ev, K.J. Friedland, H. Kostial, R. Hey, U. Jahn, E. Wiebicke, J.S. Yukecheva, V.Ya. Prinz, Phys. Rev. B **75**, 205309 (2007)
25. A.B. Vorob'ev, V.Ya. Prinz, J.S. Yukecheva, A.I. Toropov, Physica E **75**(1–2), 171–176 (2004)
26. K.J. Friedland, A. Siddiki, R. Hey, H. Kostial, A. Riedel, D. K. Maude, Phys. Rev. B **79**, 125320 (2009)
27. S. Mendach, O. Schumacher, H. Welsch, C. Heyn, W. Hansen, M. Holz, Appl. Phys. Lett. **88**, 212113 (2006)
28. V.Ya. Prinz, Microelectron. Eng. **69**, 466475 (2003)
29. V.Ya. Prinz, Physica E **23**, 260–268 (2004)
30. C. Deneke, O.G. Schmidt, Physica E **23**, 269–273 (2004)
31. C. Deneke, C.M. Muller, N.Y. Phillipp, O.G. Schmidt, Semicond. Sci. Technol. **17**, 1278 (2002)
32. O.G. Schmidt, C. Deneke, Y. Manz, C. Muller, Physica E **13**, 969 (2002)
33. P. Cendula, S. Kiravittaya, Y.F. Mei, Ch. Deneke, O.G. Schmidt, Phys. Rev. B **79**, 085429 (2009)
34. M.M.A.J. Voncken, J.J. Schermer, A.T.J. van Niftrik, G.J. Bauhuis, P. Mulder, P.K. Larsen, T.P.J. Peters, B. de Bruin, A. Klaassen, J.J. Kelly, J. Electrochem. Soc. **151**(5), G347–G352 (2004)
35. M.M.A.J. Voncken, J.J. Schermer, G.J. Bauhuis, A.T.J. van Niftrik, P.K. Larsen, J. Phys.: Cond. Matt. **16**(21), 3585–3596 (2004)
36. A.T.J. van Niftrik, J.J. Schermer, G.J. Bauhuis, P. Mulder, P.K. Larsen, J.J. Kelly, J. Electrochem. Soc. **154**(11), D629–D635 (2007)
37. R.A. Logan, F.K. Reinhart, J. Appl. Phys. **44**, 4172–4176 (1973)
38. J.J. Schermer, G.J. Bauhuis, P. Mulder, W.J. Meulemeesters, E. Haverkamp, M.M.A.J. Voncken, P.K. Larsen, Appl. Phys. Lett **76**(15), 2131–2133 (2000)
39. E. Yablonovitch, T. Gmitter, J.P. Harbison, R. Bhat, Appl. Phys. Lett. **51**(26), 2222–2224 (1987)
40. J.-I. Maeda, Y. Sasaki, N.N. Dietz, K. Shibahara, S. Yokoyama, S. Miyazaki, M.-T. Hirose, Jpn. J. Appl. Phys. **36**, 1554–1557 (1997)
41. Y. Sasaki, T. Katayama, T. Koishi, K. Shibahara, S. Yokoyama, S. Miyazaki, M. Hirose, J. Electrochem. Soc. **146**(2), 710–712 (1999)
42. M.M.A.J. Voncken, J.J. Schermer, G. Maduro, G.J. Bauhuis, P. Mulder, P.K. Larsen, Mat. Sci. Eng. **B95**, 242–248 (2002)
43. K.S.R.K. Rao, T. Katayama, S. Yokoyama, M. Hirose, Jpn. J. Appl. Phys. **39**, L457–L459 (2002)
44. L. Hollan, R. Memming, J.C. Tranchart, J. Eletrochem. Soc. **126**, 855 (1979)
45. H.S. Mavi, S.S. Islam, S. Rath, B.S. Chauhan, A.K. Shukla, Mat. Chem. Phys. **86**, 414–419 (2004)
46. B. Joshi, S.S. Islam, H.S. Mavi, V. Kumari, T. Islam, A.K. Shukla, Harsh, Physica E **41**(4), 690–694 (2009)